Geotech Geol Eng
https://doi.org/10.1007/s10706-023-02590-7

ORIGINAL PAPER

Investigating accelerated carbonation for alkali activated slag stabilized sandy soil

Hamid Reza Razeghi · Fatemeh Safaee · Armin Geranghadr · Pooria Ghadir · Akbar A. Javadi

Received: 6 March 2023 / Accepted: 16 July 2023

Abstract Portland cement as a commonly used material in soil stabilization projects, releases considerable amounts of CO_2 into the atmosphere, highlighting the need to use green binders such as ground granulated blast furnace slag as a substitute for cement. On the other side, extensive research is being conducted on accelerated carbonation treatment to decrease the industry's carbon footprint. Carbonation transforms CO_2 into carbonate minerals. This study investigates the influence of accelerated carbonation on the unconfined compressive strength (UCS) of soil stabilized with alkali-activated slag under ambient and oven curing conditions. Effects of curing time, binder content, relative density, and carbonation pressure (100, 200, and 300 kPa) were also studied. Furthermore, a calcimeter test was conducted to determine the amount of carbonate generated, which reflects CO_2 sequestration in soil. The results showed that the carbonated samples achieved higher strength than the non-carbonated samples. However, a slight decrease in UCS was observed with the increase in CO_2 pressure. The generated carbonate content directly correlated with the UCS of the samples, which explained the higher strength of carbonated samples. Also, the ambient curing condition was more favorable for the samples stabilized with GGBS, which can be attributed to the supply of required moisture. Results from XRD, SEM, and FTIR indicated that the strength development was due mainly to the formation of carbonation products ($CaCO_3$), which facilitated the densification of solidified materials.

Keywords Accelerated carbonation · Alkali-activated slag · Soil stabilization · Geopolymer · Cement

1 Introduction

In recent centuries, an increase in greenhouse gas emissions as a result of population growth and rising energy consumption has caused global climate change (Pan et al. 2016). According to estimates, the amount of CO_2 in the atmosphere rose by 31.7% between 1958 and 2021 (Wang et al. 2022). The manufacture of cement and concrete accounts for more than 5–8% of all worldwide CO_2 emissions (Li and Wu 2022; Marple et al. 2022; Suescum-Morales et al. 2022). Therefore, approaches to reduce greenhouse

H. R. Razeghi · F. Safaee · A. Geranghadr
School of Civil Engineering, Iran University of Science and Technology, Tehran 1684613114, Iran

P. Ghadir · A. A. Javadi (✉)
Department of Engineering, University of Exeter, Exeter EX4 4QF, UK
e-mail: A.A.Javadi@exeter.ac.uk

P. Ghadir (✉)
Department of Civil and Environmental Engineering, University of Strathclyde, Glasgow, UK
e-mail: Pooria.ghadir@strath.ac.uk

Published online: 31 August 2023

gas emissions and increase CO_2 sequestration have received worldwide attention (Chen et al. 2021). In particular, the 21st Global Warming Conference reached the Paris Agreement, which aims to limit the increase in global average temperature to below 1.5°C by the end of the century (Norhasyima and Mahlia 2018; Wang et al. 2019, 2022).

As a result, it is important to focus on CO_2 mitigation and reduction strategies in the cement and construction industries. Utilizing cement alternatives is one of these strategies for lowering cement usage (Chindaprasirt and Rattanasak 2019; Miraki et al. 2021). However, this substitution strategy alone has not been sufficient to reach the global CO_2 mitigation goal. Carbon sequestration is one of the potentially effective methods for lowering greenhouse gases (Mortezaei and Vahedifard 2015). Carbonation is the reaction between atmospheric CO_2 and cations in minerals (olivine, wollastonite, and serpentine) or alkaline waste (blast furnace slag, cement furnace slag, etc.) to form stable carbonates such as calcite (Chindaprasirt and Rattanasak 2019; Iorliam 2019; Kaliyavaradhan et al. 2020; Song et al. 2021; Marple et al. 2022). Calcite ($CaCO_3$) has the ability to chemically and physically bond soil particles and soil mechanical strength development (Chen et al. 2021; Romiani et al. 2021). Due to the slow speed of the natural carbonation process, high-purity CO_2 is injected into the alkaline waste in the accelerated carbonation method to boost the carbonation rate (Wang et al. 2019; Silva et al. 2021). The utilization of natural minerals can have negative environmental effects due to the mining and energy consumption required. Therefore, alkaline activated wastes (AAW) containing Ca–Mg silicates are more appropriate for soil stabilization and carbon sequestration (Chiang and Pan 2017).

Iron and steel slags, one of the possible AAW raw materials, have a higher carbonation capacity than substances like fly ash because of their higher calcium oxide content (Chiang and Pan 2017). In 2011, the iron and steel industry was responsible for roughly 22% of energy consumption and 6–7% of global CO_2 emissions (Pan et al. 2016; Chiang and Pan 2017). Vast quantities of slag are commonly stored in enormous piles, which degrades the land and pollutes the air with slag particles (Rouaiguia and El Aal 2020; Wang et al. 2020). A portion of iron and steel slag is utilized in the civil and construction industries, such as cement manufacturing, road building, and soil improvement. Despite the importance of storing and burying iron and steel slag due to its continued production in response to the rising demand for iron and steel products, not all slags have been identified as having recyclable potential (Dindi et al. 2019). Slag is recognized for its highly alkaline nature and large concentrations of metal ions, particularly calcium; hence, it can be used for carbonation in the soil to sequester and store CO_2 (Miraki et al. 2021).

The geopolymer binders are produced by activating aluminosilicate raw material in a very alkaline environment (Ghadir and Razeghi 2022). Typically, aluminosilicate precursors obtained from waste materials or natural resources do not require extensive pretreatment (Ghadir et al. 2021; Miraki et al. 2021). This type of material's mechanical strength and heat resistance is quickly attained through early hardening at ambient temperature (Aredes et al. 2015; Shariatmadari et al. 2021). These characteristics make them viable replacements for building materials based on Portland cement. Aluminosilicate raw materials contain sufficient quantities of reactive silicate and alumina (Wong et al. 2019; Razeghi et al. 2022). The geopolymerization procedure leads to the development of a hardened product composed primarily of Si, Al, and O in addition to alkali metal components such as Na and K (Naghizadeh 2019; Samadi et al. 2023). The geopolymerization procedure consists of two primary steps: initially, alumina and silica are dissolved in the alkali activator along with the surface hydration of insoluble particles (Miraki et al. 2021). After that, a gel is formed by the soluble species and active surface groups, creating a rigid inorganic polymer structure. The base of the geopolymer binder is an aluminosilicate gel network, which includes tetrahedral AlO_4 bonded to SiO_4 by shared oxygen atoms. In order to neutralize the negative charge of four coordinated Al^{-3} ions, the framework cavities contain positive ions such as Na^+ (Harichane et al. 2011; Aredes et al. 2015). Several parameters, such as the mineral composition of aluminosilicate material, alkali-activator properties, the particle size distribution of raw material, curing conditions, and water content, can influence geopolymerization mechanism (Syed et al. 2020; Shariatmadari et al. 2021). These variables influence the rate of geopolymerization, which affects the development of geopolymer cement characteristics.

The compact microstructure, improved mechanical capabilities, and volumetric stability of geopolymer-stabilized soils make them ideal for fulfilling the demand of engineered soil (Ghadir and Ranjbar 2018). Additionally, as previously mentioned, the high concentration of Ca ions in AAW, particularly in ground granulated blast furnace slag (GGBS), makes them desirable for carbonation reactions that capture CO_2 (Abdullah et al. 2019; Marple et al. 2022). In previous research, after 90 days of curing, carbonation of alkali-activated olivine-treated soil improved the soil's strength by up to 60% compared to untreated soil and by 1.5% compared to alkali-activated olivine-treated soil (Fasihnikoutalab et al. 2017). In another study, the influence of pressure variations on the CO_2 capture of slag was investigated in the range of 1.0–6.0 MPa. In the early stages of aqueous carbonation, high pressure was observed to increase the rate of carbon sequestration(Mortezaei and Vahedifard 2015). nevertheless, it had no effect on the slag's final CO_2 sequestration capacity (Ukwattage et al. 2017). Poletini's research established that the effects of pressure and CO_2 concentration on the sequestration of CO_2 by slags were interrelated (Polettini et al. 2016). Under a low pressure of 0.1 MPa, increasing CO_2 concentration from 10 to 100% accelerated CO_2 sequestration in BOF slag. However, at a high pressure of 1.0 MPa, there is no such monotonous improvement of CO_2 sequestration with increasing CO_2 concentration (Polettini et al. 2016). Microstructural investigations revealed a significant change in the surface morphology of steel slag particles after carbonation (Mo et al. 2016; Ukwattage et al. 2017). In other words, the non-carbonated steel slag's microstructure was porous and loose. However, $CaCO_3$ crystals in the form of hexagonal rods were produced in large quantities after carbonation. The $CaCO_3$ crystals, which accumulated on the surface of minerals, were the major byproduct of the accelerated carbonation of steel slag (Ko et al. 2015; Abdullah et al. 2019; Song et al. 2021).

The carbon capture and storage (CCS) technology has been the subject of considerable research in recent years (Mortezaei and Vahedifard 2015; Vishal and Singh 2015). However, fewer studies have looked into its qualitative and quantitative performance in stabilizing and modifying soils. Therefore, this investigation studied the effect of accelerated carbonation on the strength parameter of sandy soil stabilized with ground granulated blast-furnace slag (GGBS). The effect of binder content, relative density, accelerated carbonation pressure, and different curing times and conditions have been investigated in this experimental research. The unconfined compressive strength (UCS) test was conducted to measure the strength parameter, followed by the calcimeter test to quantify the amount of carbonate produced. X-ray diffraction (XRD) and Fourier transform infrared spectroscopy (FTIR) was also used to analyze the microstructural characteristics of stabilized and carbonated soil comprehensively. Furthermore, SEM–EDS analysis mapping was used to evaluate the geopolymers' matrixes.

2 Materials and methods

2.1 Soil characterization

The sandy soil used in this research was Firoozkooh sand from the Firoozkooh mine in Tehran province, Iran. Figure 1 shows the distribution curve of soil granulation according to ASTM D422-63 (ASTM D422 2007). Firoozkooh sand is classified as poorly graded sand (SP) according to the Unified Soil Classification System (USCS). Table 1 shows the physical and chemical properties (X-ray fluorescence analysis) of the sand.

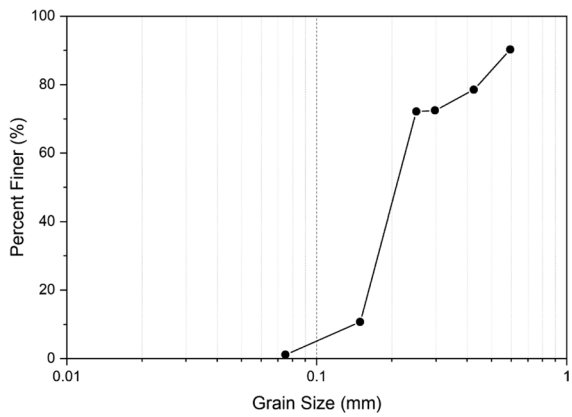

Fig. 1 Particle-size distribution of the Firoozkooh sand

Table 1 Physical and chemical properties of Firoozkooh sand

Physical properties						
γ_{dmax}	γ_{dmin}	D_{50}	D_{60}	C_u	C_c	G_s
1.63	1.41	0.25	0.27	1.8	0.98	2.67
Chemical properties						
Component	Si_2O	Al_2O_3	Fe_2O_3	CaO	Na_2O	K_2O
Percentage	95–98	0.5–1	0.5–1	0.5–1	0.02–0.5	0.5–0.7

2.2 Binders characterization

The GGBS used as a binder was obtained from the Isfahan Steel Plant located in Isfahan Province, Iran. The chemical components of GGBS obtained using X-ray fluorescence analysis are shown in Table 2.

In this study, the alkaline activator used to activate the geopolymerization reactions was sodium hydroxide (NaOH) and sodium silicate (Na_2SiO_3) in combination. Sodium hydroxide is manufactured by DRM Industrial Chemical Complex located in Tehran, Iran, and sodium silicate with silicate modulus (Ms) of 2.3 is produced in Qazvin Silicate Industries Factory in Qazvin province, Iran. Using sodium hydroxide as an alkaline activator breaks the bonds of silica and alumina in the early stages of geopolymerization. The addition of sodium silicate increases the Si/Al ratio in the geopolymer system, which results in a more effective alkaline activator (Ahmari et al. 2012; Leong et al. 2016).

3 Soil stabilization and characterization tests

3.1 Specimen preparation and mechanical characterization

In order to prepare the unconfined-uniaxial compressive test specimens, cylindrical molds of 37.5 mm in diameter by 80 mm in height were used. A ten-minute hand mixing process was used to thoroughly combine the soil with the geopolymer solution. A loading machine was used to statically compact all specimens into three equal layers, which were subsequently extruded using a Harvard Miniature Compaction Apparatus. As shown in Table 3, binder content of 10, 15, 20, and 25% of the dry soil weight was used. Calculations for alkaline activators were done with the ratios $SiO_2/Na_2O = 1$ and Na_2O/binder = 0.12 (Ahmari et al. 2012; Leong et al. 2016; Cho et al. 2017). The required amount of water was considered constant at 13.5 wt % (to dry soil) in all specimens. After sample preparation with relative densities of

Table 2 Chemical properties of GGBS

Component	SiO_2	Al_2O_3	Fe_2O_3	CaO	Na_2O	MgO	K_2O	TiO_2	MnO	SO_3
Percentage	35.9	10.35	0.55	34.31	1.4	7.73	0.99	0.86	1.62	4.57

Table 3 Program of experiments

Relative density (%)	Binder content (%)	Curing condition	Curing time (day)	CO_2 pressure (kPa)	Carbonation time (hour)
30,80	10,15,20	OC*, AC[a]	7	Atmosphere[b], 100, 200	1
30,80	25	OC, AC	7	100	1
80	20	OC, AC	7	300	1
80	20	OC, AC	3, 14	Atmosphere, 100	1

*Oven curing condition = 60 °C, relative humidity 15%

[a]Ambient curing condition = 25 °C, relative humidity 70%

[b]Non-carbonated samples

30 and 80%, initial curing was applied to each sample. All samples were exposed to two different curing conditions; oven condition (samples were put in an oven with temperature of 60 °C and relative humidity 15%) and ambient condition (samples were put in a humidity chamber with temperature of 25 °C and relative humidity 70%) for 7 days, except samples treated for 3 and 14 days to evaluate the effect of curing time. To consider the effect of curing condition in different regions with various climates, the oven condition was applied to simulate the curing condition in arid regions. Carbonated samples were exposed to accelerated carbonation at 100, 200 and 300 kPa pressure for 1 h (equilibrium time) and then compared with the non-carbonated control sample. To prevent carbonation in non-carbonated samples, the samples were put in a sealed bag after initial curing. A laboratory setup was used for the carbonation process in this study, Fig. 2. This setup consists of a cell that provides the desired CO_2 pressure for the carbonation of the samples.

A universal testing device (Digital Tritest 50/ELE) was used to measure UCS. The rate of axial strain was regulated at 1 mm/min. The average of three specimens' mechanical strength was used as the strength of specimen.

3.2 Equilibrium Time

Figure 3 shows the increase in the weight of carbonated samples during exposure to CO_2. On the assumption that all of the injected CO_2 reacts entirely with GGBS, the amount of CO_2 intake can roughly indicate the amount of carbonation products, which will aid in explaining how UCS evolved. Given the prolonged hydration of GGBS, CO_2 absorption is the primary cause of the little weight gain of solidified samples exposed to CO_2 carbonation (Wang et al. 2019). Figure 3 shows that the weight of the samples continued to grow for up to 60 min, which indicates that the samples had absorbed carbon dioxide. The weight of the sample is nearly set after 60 min. Thus, that amount of time is sufficient for carbonation. All carbonated samples are treated to CO_2 pressure for one hour in the accelerated carbonation cell.

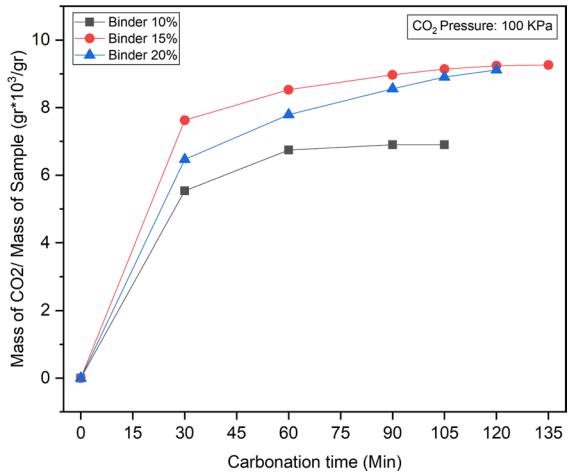

Fig. 3 Evolution of CO_2 absorption amount with carbonation time

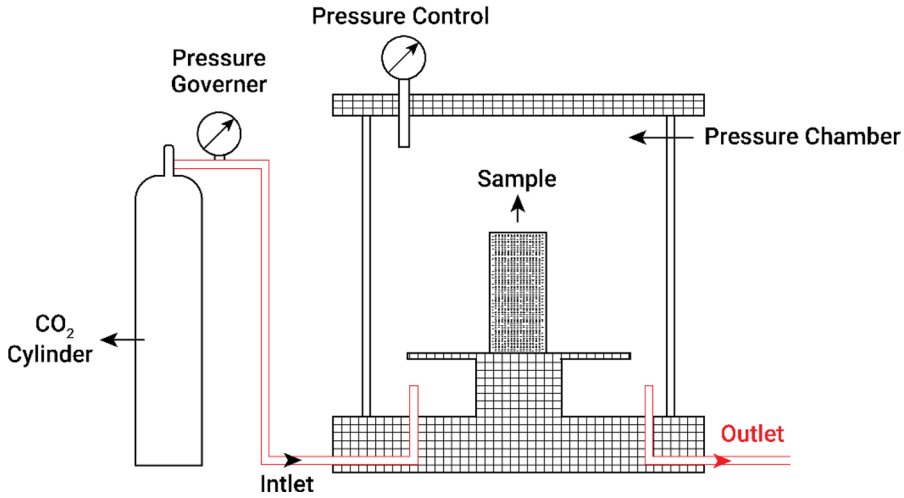

Fig. 2 Schematic diagram of carbonation apparatus

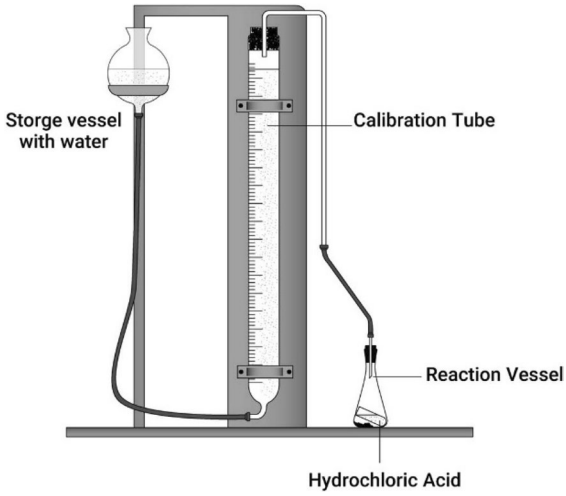

Fig. 4 Calcimeter instrument

3.3 Calcimeter test

Calcimeter test was performed on carbonated treated samples to determine the amount of $CaCO_3$. The calcimeter is an instrument for measuring the amount of carbonate in soil (Fig. 4). In this technique, a volumetric approach determines the amount of carbonates in a sample; the gas volume of CO_2 produced by the reaction between soil and hydrochloric acid is used to calculate the $CaCO_3$ content. In this investigation, the amount of inorganic carbonate present in the carbonated treated samples was quantified using a calcimeter, and the results were compared to those of the non-carbonated treated samples. The test was performed using a calcimeter according to the standard ISO 10693(1995E) (2014).

3.4 Microstructural characterization

The alkali-activated GGBS stabilized soil samples were analyzed by X-ray diffraction (XRD) utilizing a Panalytical Company X'Pert Pro device with a Cu anode material, a 2θ range of 5–85° performed at 40 kV and 40 mA. The powder materials were compressed into KBr pellets for FTIR analysis using a PerkinElmer Company FTIR spectrometer instrument. The Scanning Electron Microscopy (SEM) setup (TESCAN vega 3, Czech Republic) was used in the backscattered electron (BSE) mode at 20 kV accelerating voltage in a high vacuum condition. To determine the elemental analysis of the specimens, EDS at 20 kV fully incorporated into the TESCAN system was utilized.

4 Results and analysis

4.1 Compressive strength

The influence of parameters such as carbonation pressure, binder to soil ratio, relative density, and different curing conditions and times on compressive strength were investigated. The results show that the carbonated samples achieved higher compressive strength than the non-carbonated samples.

Figure 5 depicts compressive strength development for carbonated specimens under various CO_2 pressures, varied binder contents, and different relative densities under two curing conditions. The samples were carbonated for an hour following 7-day initial curing period in oven or ambient temperature. Carbonated samples were subjected to CO_2 at pressures of 100, 200, and 300 kPa and then compared with non-carbonated samples to investigate the effect of carbonation pressure on mechanical strength of specimens. Noteworthy, zero pressure denotes non-carbonated samples. In general, samples under carbonation achieved higher compressive strength than non-carbonated samples. At a relative density of 80% and a binder content of 20% in the OC and AC conditions, the compressive strength of non-carbonated samples increased from 6.7 and 10.81 MPa to 12.14 and 15.11 MPa in samples with 100 kPa carbonation pressure, respectively.

Previous research showed that a greater CO_2 pressure is generally helpful to the dissolving of CO_2 in water to generate carbonate (CO_3^{2-}) or bicarbonate (HCO_3^-), which may improve the carbonation degree (Song et al. 2021). As a result, it is anticipated that, under situations where other variables remain constant, an increase in CO_2 pressure will lead to a higher carbonation degree and, consequently, a rise in the compressive strength. However, the findings demonstrate that strength decreases slightly as carbonation pressure is raised to 200 and 300 kPa. The explanation for this adverse effect may be that

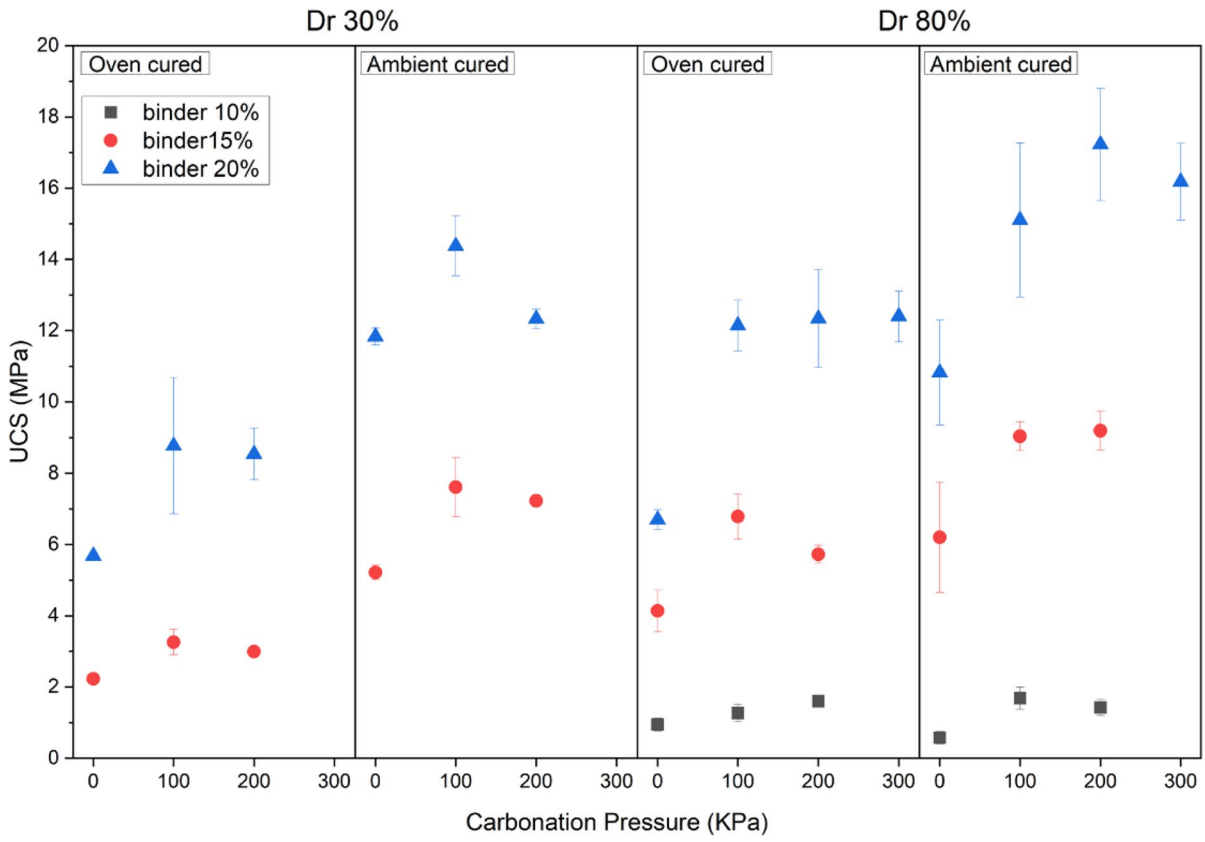

Fig. 5 Compressive strength of carbonated and non-carbonated specimens at ambient and oven curing conditions with different binder contents and relative densities

increasing CO_2 pressure prompts rapid precipitation of carbonate minerals, which leads to a faster obstruction of slag pores and a quicker production of protective carbonate coatings on the grain surface, hindering contact between slag and CO_2 (Polettini et al. 2016; Song et al. 2021; Li and Wu 2022).

As shown in Fig. 5, compressive strength has been improved by adding more slag, from 10 to 15 and finally 20%, in samples with relative densities of 30% and 80% under various curing conditions for carbonated and non-carbonated samples. The chemical composition of ground blast furnace slag is the cause of this rise in UCS. Calcium oxide, which composes 34% of the GGBS chemical structure, is crucial for absorbing carbon dioxide and forming carbonates, which boosts soil stability (Song et al. 2021). As a result, there is increased UCS due to more calcium. Furthermore, the soil's mechanical properties have been enhanced by the coexistence of sodium aluminosilicate gel, a product of geopolymerization, and calcium silicate hydrate gel, which is brought on by the presence of calcium (Ghadir and Razeghi 2022). In other words, activating high-calcium slag includes calcium dissolving and aluminum's participation in forming C–(A)–S–H gel, which raises compressive strength. However, the major reaction product in these systems is sodium aluminosilicate gel. This three-dimensional N–A–S–H gel increases strength because of alkaline activation of the aluminosilicate gel (Phoo-Ngernkham et al. 2015; Miraki et al. 2021).

In addition to 7-day, 3-day and 14-day samples were prepared to evaluate the influence of curing time on compressive strength and the effect of carbonation at various ages. Figure 6 demonstrates that under both OC and AC curing conditions, the growth in compressive strength was maintained until 14 days at atmospheric pressure. However, the rate of strength

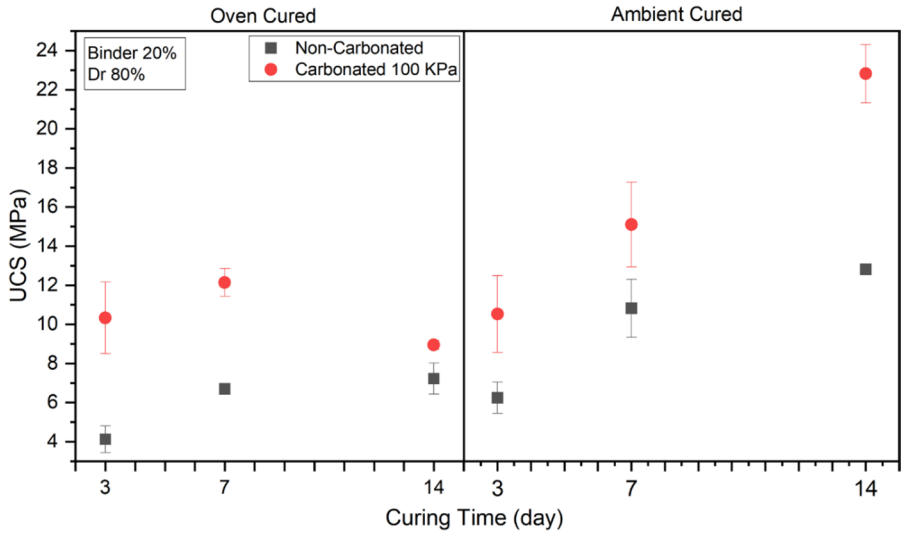

Fig. 6 Compressive strength of non-carbonated and carbonated samples at different curing times and conditions for 20% binder and 80% relative density

development of non-carbonated samples was substantially higher until 7 days and subsequently decreased. Samples were carbonated under 100 kPa after being cured for 3, 7, or 14 days. Accelerated carbonation has caused a considerable increase in compressive strength in samples of all ages and ambient condition. While at 14 days under oven curing condition, the effect of carbonation on UCS has diminished, resulting in a drop in compressive strength relative to the 7-day carbonated sample. This can be attributed to the role of moisture in the carbonation reaction; because accelerated carbonation mimics natural weathering, CO_2 combines with metal-oxide in the presence of water to speed up the reaction (Pan et al. 2016; Chiang and Pan 2017). In oven condition, with increasing curing time, the sample's moisture content decreases; that is why the effect of carbonation process has reduced after 14 days of curing in dry condition. Two curing conditions (OC and AC) were examined in this study, and the outcomes of each are displayed separately in Figs. 5 and 6. The ambient condition, which includes a temperature and relative humidity of 25 ℃ and 70%, respectively, are more favorable for curing GGBS and achieving a higher compressive strength (Miraki et al. 2021). Similar results were observed in previous research. In the study by Bilim et al., the GGBS mortars that were cured at 23 ± 2 °C and 95% relative humidity showed the best results (Bilim et al. 2013). Conversely, low relative humidity and dry curing condition resulted in the lowest curing performance for GGBS mortars' mechanical properties (Bilim et al. 2013). Numerous studies have demonstrated that the incorporation of GGBS into soil enhances its strength at ambient temperature. This can be attributed to the heightened formation of CSH gel within the modified soil structure, which is facilitated by the amorphous phase of the GGBS binder. Furthermore, curing the GGBS-modified soil at ambient temperature improves the formation of aluminosilicate gel within the sample, further contributing to its strength. In contrast, subjecting the modified soil to a high temperature of 60 ℃ has been shown to decrease its strength. This phenomenon can be linked to the loss of structural water, a crucial factor in facilitating the geopolymerization process (Miraki et al. 2021).

4.2 Calcimeter Test

The carbonates formed due to CO_2 absorption were the reason for the carbonated samples' increased compressive strength than non-carbonated samples. The amount of carbonate produced in the chosen samples was measured using the calcimeter test. The samples' variations in carbonate content and their relationship to UCS based on carbonation pressure, binder content, relative density, and curing time are shown in Figs. 7 a, b, c, d, respectively.

In Fig. 7a, to study the effect of carbonation on the carbonate content, the curing time of 7 days, the binder content of 20%, and the relative density of 80% were considered constant. Under both curing

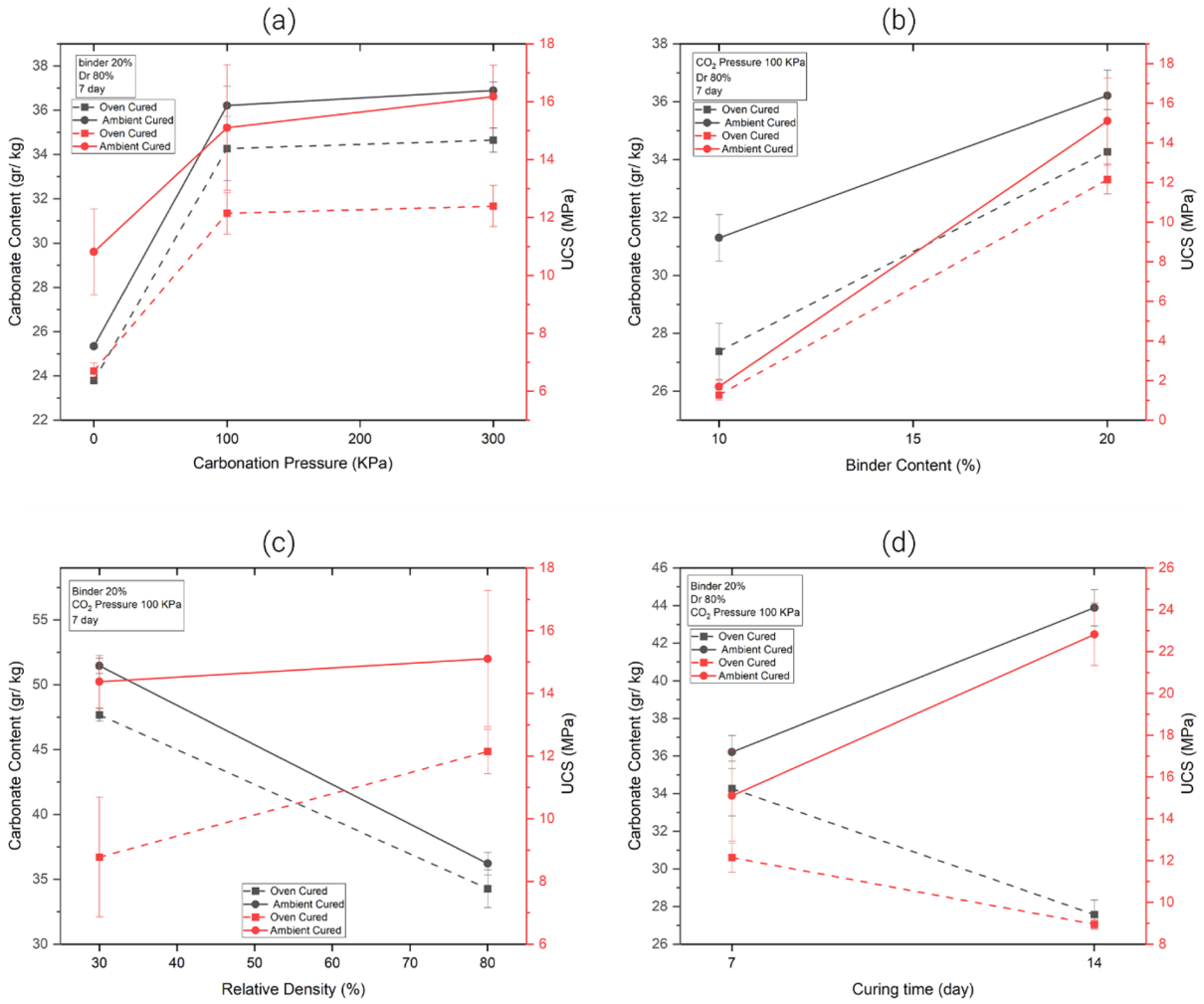

Fig. 7 Variations of carbonate content and UCS based on: **a** Carbonation pressure; **b** Binder content; **c** Relative density; **d** Processing time

conditions, the amount of carbonate formed in the carbonated samples is greater than in the non-carbonated samples. However, compared to the pressure of 100 kPa, the amount of carbonate generated at 300 kPa has altered slightly. The higher UCS of carbonated samples is attributable to the carbonate generated by CO_2 absorption. Meanwhile, increasing carbonation pressure did not affect the growth in carbonate content and UCS.

The binder content effect on the carbonate content and UCS is demonstrated in the 7-day samples with an 80% relative density, as shown in Fig. 7b, under a constant carbonation pressure of 100 kPa. GGBS is a calcium-rich binder, which participates in the carbonation reaction, so increasing the amount of binder increases the carbonate content and UCS of the samples (Song et al. 2021). As shown in Fig. 7c, carbonate content in the sample structure with a density of 30% is considerably greater than that of 80%. In other words, the maximum carbonate content measured corresponds to samples with a Dr of 30%. This is due to the presence of more voids in the structure of 30% relative density samples, which permits greater CO_2 penetration into the structure of the stabilized sample. However, as expected, the compressive strength of denser samples is greater.

The effect of accelerated carbonation in the 14-day samples is significant in ambient condition, as was

discussed in the previous section. In contrast, the effect of carbonation diminishes in oven condition as the initial curing time increases. Figure 7d shows that as the initial curing time increases, the amount of carbonate generated in the sample under carbonation of 100 kPa and its compressive strength increase. However, according to the trend of the UCS diagram, under oven condition, the amount of carbonate generated in a 14-day curing sample is smaller than 7-days. This shows that increasing the initial curing time can reduce the effect of accelerated carbonation. The carbonate content measured in the samples cured in ambient conditions is higher than under oven conditions, which is also supported by the results of the uniaxial strength test, as shown in all Figs. 7a, b, c, d for the identical samples under different curing conditions.

4.3 FTIR Test

The FTIR spectra of non-carbonated and carbonated samples at various pressures, curing times and conditions, and relative densities are shown in Fig. 8. The strong peak formed in the range of 3400–3500 cm^{-1}, attributed to the stretching vibration of OH–, is associated with water (Chen and Gao 2019; Syed et al. 2020). This water is either absorbed on the surface material or trapped in the holes of the geopolymer structure. Additionally, the small peaks seen in the 1600–1700 cm^{-1} range are due to the bending vibration of OH– (Miraki et al. 2021; Santos et al. 2021). The absorption bands that occurred at wavenumbers between 1410 and 1458 cm^{-1} indicate the asymmetric tensile bonds of O–C–O, which are often generated by the carbonation of geopolymeric materials

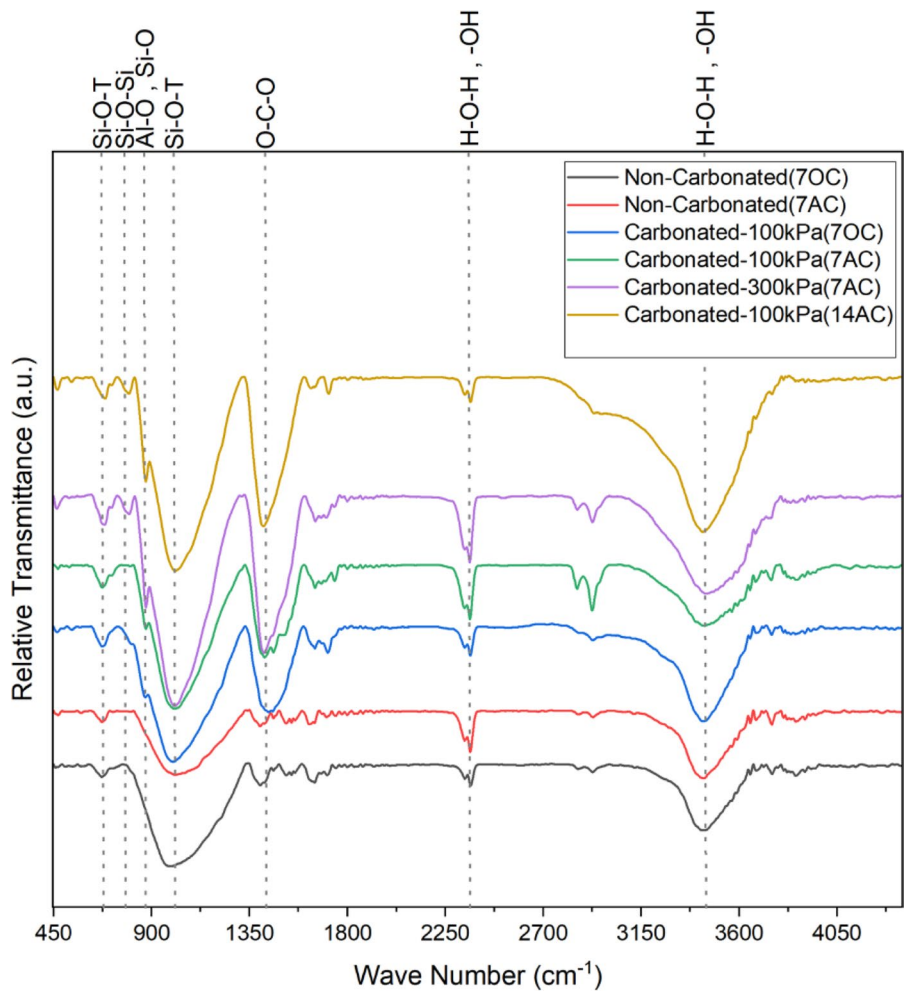

Fig. 8 FTIR spectra of the carbonated and non-carbonated samples

(Chen and Gao 2019; Miraki et al. 2021). This shows the presence of carbonate (CO_3^{-2}) associated with calcite ($CaCO_3$ polymorph) in the sample structure (Fasihnikoutalab et al. 2017; Santos et al. 2021). In the spectrum of non-carbonate samples, there is no distinct peak in the range of 1410 cm^{-1}. However, when these samples are subjected to carbonation, the intensity of the peak in this range, which corresponds to the O–C–O bond in carbonates, increases significantly. This increase was attributed to the development of carbonates like calcite in the sample's structure as a result of accelerated carbonation and CO_2 pressure.

The absorption bands appearing between 980 and 1100 cm^{-1} correspond to bending vibrations of Si–O bonds in tetrahedral Si–O, symmetric vibrations in Si–O–Si bonds, and stretching vibrations in Si–O–Al bonds in C–S–H gel (Antunes Boca Santa et al. 2013; Jha et al. 2020). This absorption band, which is introduced as the essential properties of the molecular structure of geopolymer, is abundant in the FTIR spectra of aluminosilicate materials (Antunes Boca Santa et al. 2013; Chen and Lu 2015; Adak et al. 2017; Fasihnikoutalab et al. 2017; Miraki et al. 2021; Santos et al. 2021). Because Si–O bonds are stronger than Al–O bonds, AlO_4 tetrahedral structures have been replaced by SiO_4 as a result of the expansion of geopolymerization reactions and the creation of the interconnected geopolymer network. This has caused this band to shift to lower wavelengths (Antunes Boca Santa et al. 2013; Santos et al. 2021). Al–OH, Al–O bond stretching, and Si–O vibration stretching were related to bands at 914, 790–730, and 680–650 cm^{-1}, respectively (Chen and Lu 2015; Adak et al. 2017; Fasihnikoutalab et al. 2017; Miraki et al. 2021; Santos et al. 2021).

4.4 XRD Test

Figure 9 shows the XRD patterns of carbonated and non-carbonated samples with 20% slag treated in ambient conditions for 7 days. Amorphous background signals predominate over crystalline signals in all XRD patterns, which is indicative of the materials' primarily amorphous nature (Santos et al. 2021; Marple et al. 2022). The sand primarily consisted of the mineral quartz (Q, PDF# 01-087-2096), which was caught at the 2θ value of 26.6° identified in all samples (Park et al. 2020). A little fraction of calcite

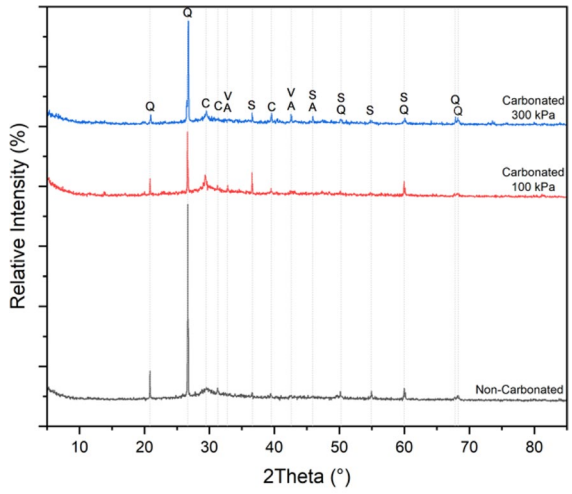

Q: quartz, C: calcite, A: aragonite, V: vaterite, S: spurrite

Fig. 9 XRD patterns of non-carbonated and carbonated samples with the pressure of 100 and 300 kPa for treated soil with 20% slag and 80% relative density, cured at ambient condition for 7 days

(C, PDF# 00-003-0596) was identified in the non-carbonated sample due to natural carbonation by atmospheric CO_2. No other $CaCO_3$ polymorphs, such as vaterite or aragonite, were found in the non-carbonated sample. In carbonated samples, the intensity of peaks associated with calcite has increased, particularly at the $2\theta = 29.5°$, which suggests the generation of more carbonate in the presence of CO_2 pressure. In addition, the peaks related to aragonite (A, PDF# 01-071-2396), vaterite (V, PDF# 00-033-0268), and spurrite (S, PDF# 00-004-0640) can be distinguished in these samples.

$CaCO_3$ polymorphs (calcite, aragonite, and vaterite) precipitate preferentially based on reaction time, carbonation degree, and the presence of other chemicals (Liu and Meng 2021). Nevertheless, calcite is the most stable calcium carbonate polymorph (Chiang and Pan 2017). In this context, it is anticipated that calcite will be the predominant $CaCO_3$ polymorph in the advanced stages of carbonation, formed by the precipitation and transformation of other calcium carbonate compounds (amorphous, vaterite, and aragonite) (Park et al. 2020; Santos et al. 2021). As seen in Fig. 10, the peaks associated to calcite, aragonite, and vaterite become increasingly pronounced with increasing curing time. Additionally, it can be deduced from the XRD patterns of the samples cured

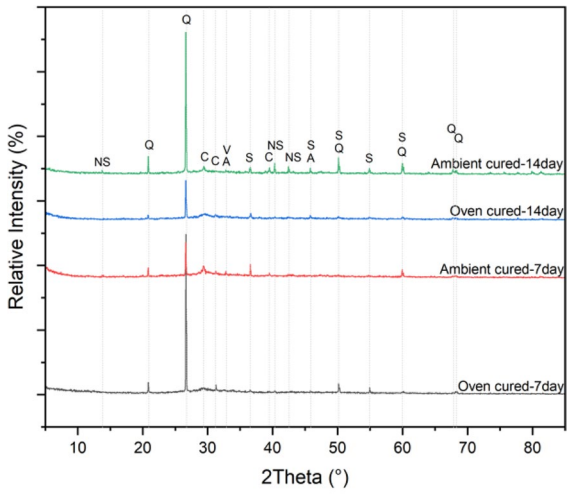

Q: quartz, C: calcite, A: aragonite, V: vaterite, S: spurrite, NS: N-A-S-H, CS: C-S-H

Fig. 10 XRD patterns of carbonated 20% slag and 80% relative density treated soil at different curing times and conditions

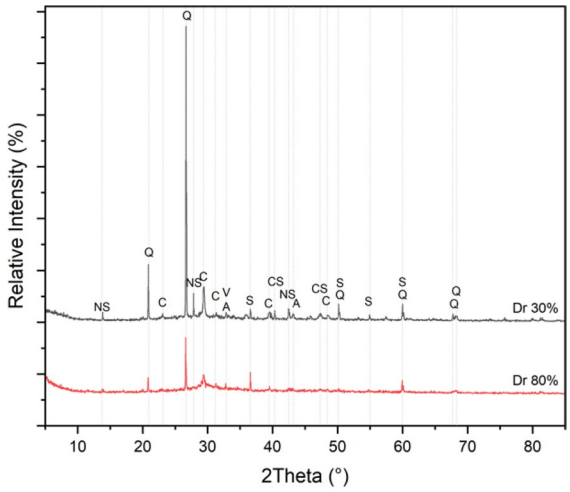

Q: quartz, C: calcite, A: aragonite, V: vaterite, S: spurrite, NS: N-A-S-H, CS: C-S-H

Fig. 11 XRD pattern of carbonated stabilized soil (20% GGBS) cured at ambient condition for 7 days, with different relative densities

under ambient and oven conditions that curing under ambient condition results in the generation of greater geopolymerization and carbonation products.

Figure 11 depicts the pattern of two carbonated samples aged under ambient conditions for seven days with relative densities of 30% and 80%. It is clear that the peaks related to the polymorph of calcium carbonate crystals, such as calcite, aragonite, and vaterite, are more intense in the sample, with a relative density of 30%. In addition, N–A–S–H (NS, PDF# 00-012-0228) and C–S–H (CS, PDF# 01-081-1987) gels have been detected at a relative density of 30%, which is a confirmation of the formation of geopolymerization products in the sample. Sodium aluminosilicate hydrate (N–A–S–H) and calcium silicate hydrate (C–S–H) were produced by the alkaline activation of slag. (N, C)–A–S–H gel has a high silica content (Sivapullaiah and Jha 2014). It is composed of a blend of crystalline and amorphous structures, which contributes to mechanical strength development and compacted microstructure density of specimens (Ghadir and Razeghi 2022). The sample with 30% relative density contains more voids than the sample with 80% relative density, making it more susceptible to CO_2 absorption in the form of carbonates and geopolymerization products. According to the calcimeter test, the amount of carbonate recorded is 51.5 g per kg of GGBS-stabilized soil, which can be a proof for the high carbon capture potential of slag.

4.5 SEM–EDS characterization

The SEM images of carbonated and non-carbonated samples with a 20% binder content are shown in Fig. 12. Selected samples have been cured in ambient conditions.

In Fig. 12a, adding activated slag to the soil results in the creation of aluminosilicate gel, which binds the soil particles together, hence increasing the soil's strength. EDS elemental analysis reveals the presence of calcium, aluminum, silicon, and sodium in the arrow-marked region of the sample structure, which suggests the production of C–(A)–S–H and N–(A)–S–H gels (Arabi et al. 2016). However, certain voids and cracks are detected in the sample's structure before carbonation, and the circle in the picture marks some unreacted slag. In contrast, in the carbonated sample (Fig. 12b), the carbonation pressure accelerated the reaction and created a smooth and dense surface. The elemental analysis of this sample reveals a higher proportion of carbon, which overlaps with a higher quantity of calcium, indicating the creation of more carbonates in the carbonated sample (Chiang and Pan 2017; Praneeth et al. 2020). In the carbonated sample with a relative density of 30% (Fig. 12c), more carbonate crystals are observed. These formations are typical

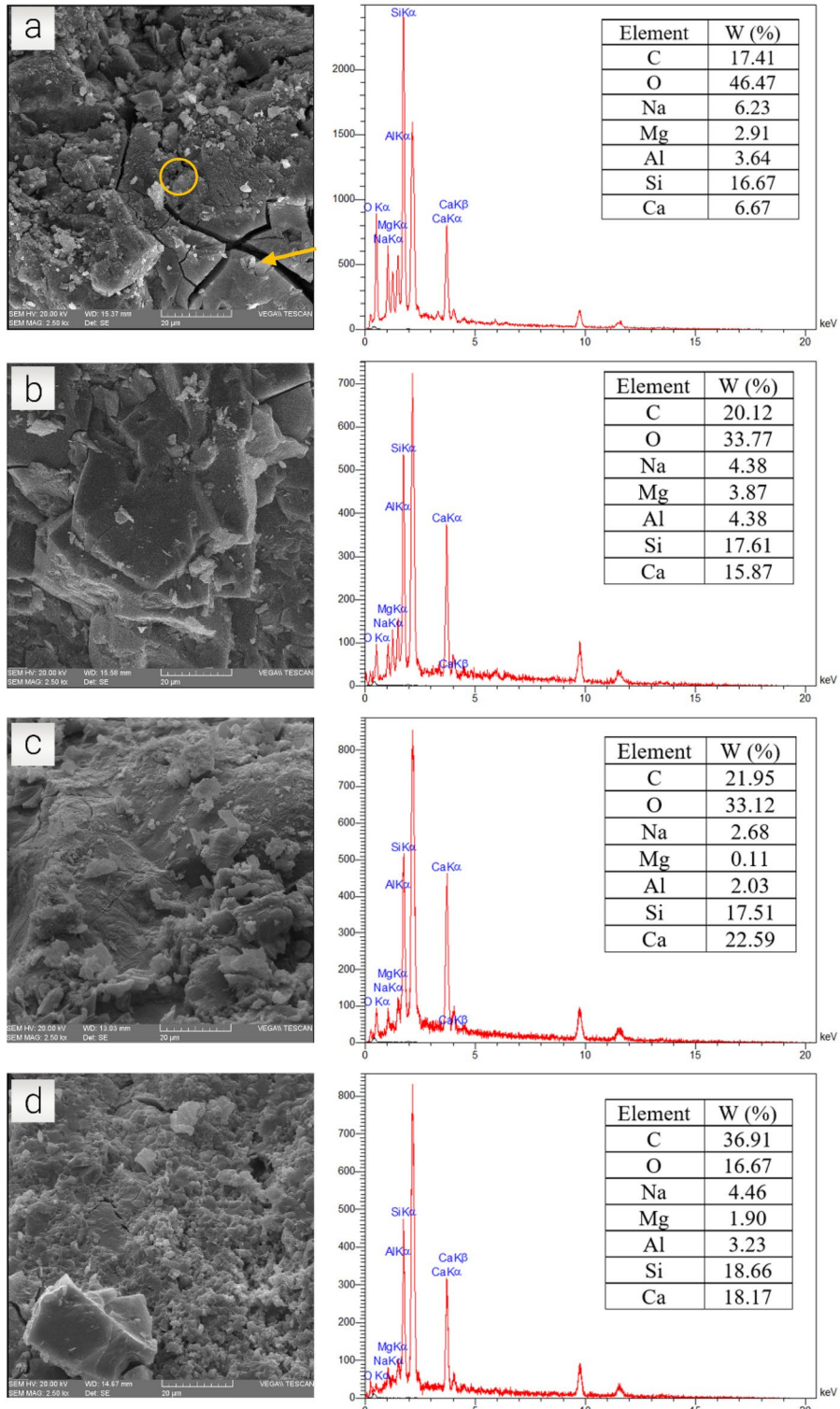

Fig. 12 SEM micrographs and EDX analysis of **a** 20% non-carbonated sample after 7 days ambient curing, **b** 20% carbonated sample after 7 days ambient curing, **c** 20% carbonated sample with Dr 30% after 7 days ambient curing, **d** 20% carbonated sample after 14 days ambient curing

of $CaCO_3$, which is supported by EDS spectra that show carbon (C), oxygen (O), and calcium (Ca) peaks. The carbon peak of the carbonated pattern grew dramatically, according to EDS analysis [10]. Calcite, aragonite, and vaterite were also found in the carbonated sample by XRD. Typically, calcite crystals are rhombohedral, prismatic, or scalenohedral, whereas aragonite crystals are needle-like. In nature, calcium carbonate can be found in two different shapes: hexagonal (as calcite) and orthorhombic (as aragonite) (Chiang and Pan 2017). These results support the high strength of samples with a relative density of 30% (almost the same as samples with a density of 80%). Figure 12d demonstrates that in ambient condition, as curing time increases, more carbonates are generated, resulting in a denser structure than the 7-day sample. The EDS analysis reveals a substantial increase

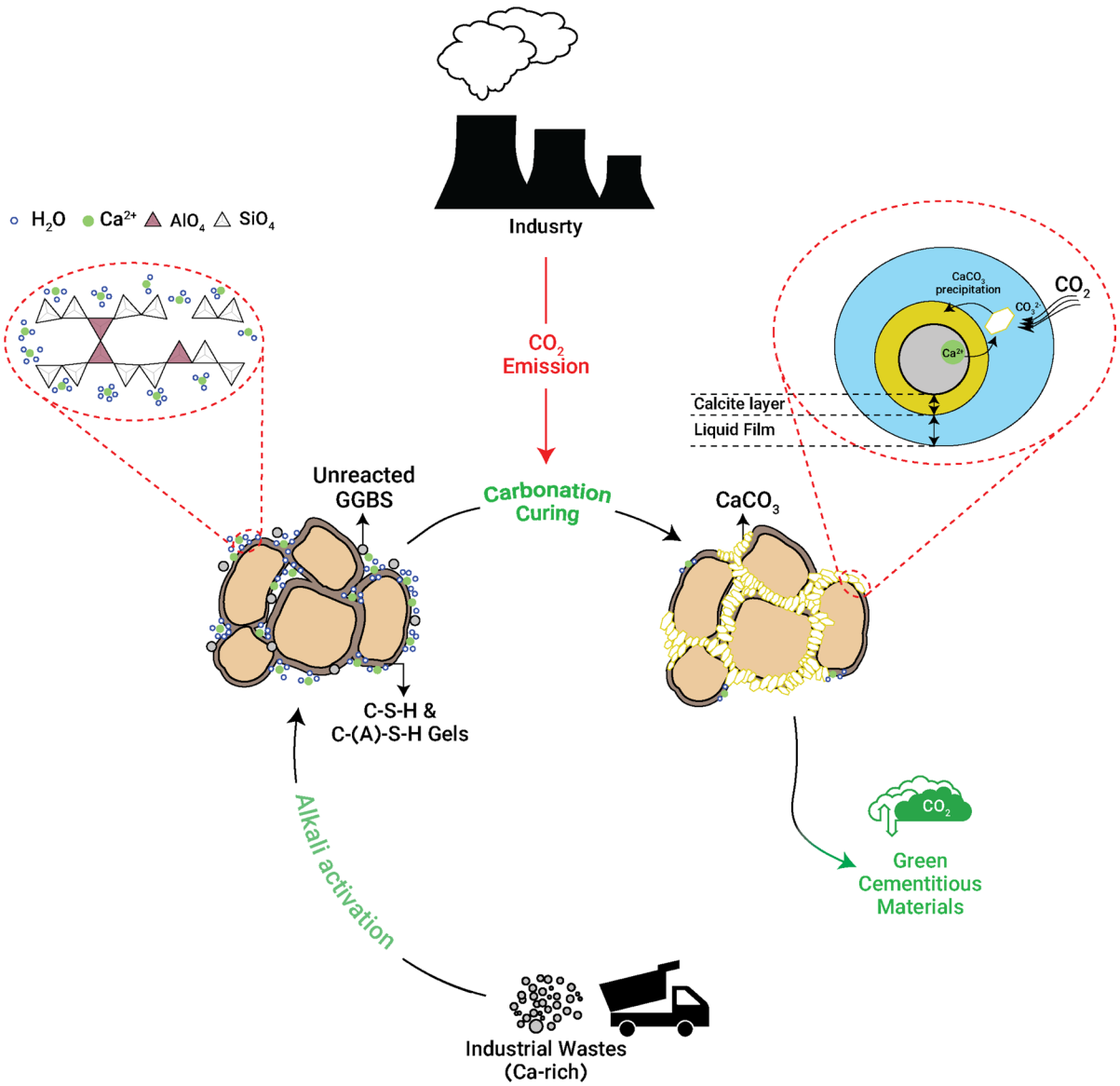

Fig. 13 Schematic diagram of accelerated carbonation using alkali activation of industrial wastes

in the amount of carbon compared to the 7-day sample, confirming the development of carbonates.

5 Discussion

The conceptual diagram of accelerated carbonation using alkali activation of soild wastes is shown in Fig. 13. This environmentally friendly method provides the opportunity to convert gaseous CO_2 into solid carbonates, so that we can achieve a sustainable way to control CO_2 emissions. Additionally, after carbonation, the chemical and physical characteristics of industrial wastes could be improved, allowing for their reuse in a range of engineering applications as green building materials (e.g., supplementary cementitious materials) (Fernández Bertos et al. 2004; Chiang and Pan 2017).

The alkali activation process occurs during the initial preparation of alkaline wastes. The alkali activator solution breaks Si–O and Al–O bonds in GGBS throughout the reaction process, resulting in mechanical strength development via the creation of calcium silicate hydrate (C–S–H) and calcium aluminate silicate hydrate (C–A–S–H) gels (Miraki et al. 2021). During the accelerated carbonation process, The gaseous CO_2 is dissolved into the moisture present in the sample and turned into carbonate ions (CO_3^{2-}). Calcium oxide and magnesium oxide, which exist in most industrial wastes, are the best metal oxides to react with CO_2 (Chiang and Pan 2017). In the presence of aqueous conditions, the carbonate ions react with the Ca^{2+} ions to form carbonate precipitates (Yi et al. 2020). Carbonates crystallize on the surface of the particle and form a calcite layer (Chiang and Pan 2017; Reddy et al. 2019; Song et al. 2021; Li and Wu 2022). In extremely severe carbonation procedures, the reaction advances and the CO_2 combines with the C–S–H gel to produce $CaCO_3$ and silica gel (Puertas and Palacios 2007). The influence of water in the carbonation reaction was mentioned in the literature (Fernández Bertos et al. 2004; Kim and Kwon 2019). In gaseous state, CO_2 does not react with calcium-based substances effectively. Carbon dioxide needs to be dissolved in water to generate carbonic acid (H_2CO_3). However, a large amount of water causes the carbonation process to be inefficient (Kim and Kwon 2019). According to Fig. 13, when the water volume increased, the diffusion length of H_2CO_3 from the water's surface to the calcium-based materials also increased (Kim and Kwon 2019). The precipitation of calcite particles causes the formation of the calcite layer, which acts as a deterrent to the more leaching of calcium. As a result, Ca^{2+} required for the carbonation reaction is not supplied (Li and Wu 2022).

6 Conclusions

This research studied the potential of using alkali-activated GGBS as a green binder in soil stabilization projects. In addition, it investigated the effect of accelerated carbonation on the mechanical and microstructural properties of stabilized soil with alkali-activated slag. Based on the results, the following conclusions are drawn.

- GGBS was effective for stabilizing sandy soil, and by increasing the binder content to 20% of the dry weight of the soil, the UCS increased.
- Accelerated carbonation with the development of carbonation products such as calcium carbonates in the stabilized soil structure increases the compressive strength; however, the pressure of 100 kPa was sufficient for carbonation; expanding the carbonation pressure had a negative effect on mechanical strength development.
- GGBS is highly reactive at ambient temperature, and humidity plays a vital role in the formation of carbonation products, so the effect of accelerated carbonation on the sample 14 days-cured samples in oven condition was reduced.
- The calcimeter results' trend is similar to the UCS test, so the increase in samples' strength is attributed to the amount of carbonate formed in its structure.
- The highest carbonate content is related to the sample with a relative density of 30% due to more pores and the possibility of more CO_2 penetration in its structure.
- The FTIR, XRD, and SEM–EDS-mapping microstructure tests show the formation of geopolymer gels and carbonate in the samples.

Acknowledgements The authors would like to appreciate the efforts of Professor Nader Shariatmadari (RIP). This study was supported by MatSoil Company (No. 04L/2023). This research was funded by the European Union's Horizon 2020 research and innovation programme under the Marie Sklodowska-Curie, Grant Number [778120].

Data availability Data is available if it is requested.

Declarations

Conflict of interest The authors declare no conflict of interest.

References

Abdullah HH, Shahin MA, Sarker P (2019) Use of fly-ash geopolymer incorporating ground granulated slag for stabilisation of kaolin clay cured at ambient temperature. Geotech Geol Eng 37:721–740. https://doi.org/10.1007/s10706-018-0644-2

Adak D, Sarkar M, Mandal S (2017) Structural performance of nano-silica modified fly-ash based geopolymer concrete. Constr Build Mater 135:430–439. https://doi.org/10.1016/j.conbuildmat.2016.12.111

Ahmari S, Zhang L, Zhang J (2012) Effects of activator type/concentration and curing temperature on alkali-activated binder based on copper mine tailings. J Mater Sci 47:5933–5945. https://doi.org/10.1007/s10853-012-6497-9

Antunes Boca Santa RA, Bernardin AM, Riella HG, Kuhnen NC (2013) Geopolymer synthetized from bottom coal ash and calcined paper sludge. J Clean Prod 57:302–307. https://doi.org/10.1016/j.jclepro.2013.05.017

Arabi N, Chelghoum N, Jauberthie R et al (2016) Formation of C-S-H in calcium hydroxide–blast furnace slag–quartz–water system in autoclaving conditions. Adv Cem Res 27:153–162

Aredes FGM, Campos TMB, MacHado JPB et al (2015) Effect of cure temperature on the formation of metakaolinite-based geopolymer. Ceram Int 41:7302–7311. https://doi.org/10.1016/j.ceramint.2015.02.022

ASTM D422 (2007) Standard test method for particle-size analysis of soils. Astm D422-63:1–8

Bilim C, Karahan O, Atiş CD, Ilkentapar S (2013) Influence of admixtures on the properties of alkali-activated slag mortars subjected to different curing conditions. Mater Des 44:540–547. https://doi.org/10.1016/j.matdes.2012.08.049

Chen T, Gao X (2019) Effect of carbonation curing regime on strength and microstructure of Portland cement paste. J CO2 Util 34:74–86. https://doi.org/10.1016/j.jcou.2019.05.034

Chen YH, Lu DL (2015) CO_2 capture by kaolinite and its adsorption mechanism. Appl Clay Sci 104:221–228. https://doi.org/10.1016/j.clay.2014.11.036

Chen T, Bai M, Gao X (2021) Carbonation curing of cement mortars incorporating carbonated fly ash for performance improvement and CO_2 sequestration. J CO2 Util 51:101633. https://doi.org/10.1016/j.jcou.2021.101633

Chiang PC, Pan SY (2017) Carbon dioxide mineralization and utilization. Springer, Singapore, pp 1–452. https://doi.org/10.1007/978-981-10-3268-4/COVER

Chindaprasirt P, Rattanasak U (2019) Characterization of porous alkali-activated fly ash composite as a solid absorbent. Int J Greenhouse Gas Control 85:30–35. https://doi.org/10.1016/j.ijggc.2019.03.011

Cho YK, Yoo SW, Jung SH et al (2017) Effect of Na2O content, SiO_2/Na_2O molar ratio, and curing conditions on the compressive strength of FA-based geopolymer. Constr Build Mater 145:253–260. https://doi.org/10.1016/j.conbuildmat.2017.04.004

Dindi A, Quang DV, Vega LF et al (2019) Applications of fly ash for CO_2 capture, utilization, and storage. J CO2 Util 29:82–102. https://doi.org/10.1016/j.jcou.2018.11.011

dos Santos VHJM, Pontin D, Ponzi GGD et al (2021) Application of fourier transform infrared spectroscopy (FTIR) coupled with multivariate regression for calcium carbonate ($CaCO_3$) quantification in cement. Constr Build Mater. https://doi.org/10.1016/j.conbuildmat.2021.125413

(2014) DIN EN ISO 10693 Soil quality-determination of carbonate content-volumetric method.

Fasihnikoutalab MH, Asadi A, Unluer C et al (2017) Utilization of alkali-activated olivine in soil stabilization and the effect of carbonation on unconfined compressive strength and microstructure. J Mater Civ Eng 29:06017002. https://doi.org/10.1061/(asce)mt.1943-5533.0001833

Fernández Bertos M, Li X, Simons SJR et al (2004) Investigation of accelerated carbonation for the stabilisation of MSW incinerator ashes and the sequestration of CO_2. Green Chem 6:428–436. https://doi.org/10.1039/b401872a

Ghadir P, Ranjbar N (2018) Clayey soil stabilization using geopolymer and Portland cement. Constr Build Mater 188:361–371. https://doi.org/10.1016/j.conbuildmat.2018.07.207

Ghadir P, Razeghi HR (2022) Effects of sodium chloride on the mechanical strength of alkali activated volcanic ash and slag pastes under room and elevated temperatures. Constr Build Mater 344:128113. https://doi.org/10.1016/j.conbuildmat.2022.128113

Ghadir P, Zamanian M, Mahbubi-Motlagh N et al (2021) Shear strength and life cycle assessment of volcanic ash-based

geopolymer and cement stabilized soil: a comparative study. Transp Geotech 31:100639. https://doi.org/10.1016/j.trgeo.2021.100639

Harichane K, Ghrici M, Kenai S, Grine K (2011) Use of natural pozzolana and lime for stabilization of cohesive soils. Geotech Geol Eng 29:759–769. https://doi.org/10.1007/s10706-011-9415-z

Iorliam YA (2019) Carbon capture potential in modified soil

Jha AK, Kumar D, Sivapullaiah PV (2020) Influence of fly ash on geotechnical behaviour of red mud: a micro-mechanistic study. Geotech Geol Eng 38:6157–6176. https://doi.org/10.1007/s10706-020-01425-z

Kaliyavaradhan SK, Ling TC, Mo KH (2020) CO_2 sequestration of fresh concrete slurry waste: optimization of CO_2 uptake and feasible use as a potential cement binder. J CO2 Util 42:101330. https://doi.org/10.1016/j.jcou.2020.101330

Kim JH, Kwon WT (2019) Semi-dry carbonation process using fly ash from solid refused fuel power plant. Sustainability (switzerland). https://doi.org/10.3390/su11030908

Ko M, Chen Y, Jiang J (2015) Accelerated carbonation of basic oxygen furnace slag and the effects on its mechanical properties. Constr Build Mater 98:286–293. https://doi.org/10.1016/j.conbuildmat.2015.08.051

Leong HY, Ong DEL, Sanjayan JG, Nazari A (2016) The effect of different Na_2O and K_2O ratios of alkali activator on compressive strength of fly ash based-geopolymer. Constr Build Mater 106:500–511. https://doi.org/10.1016/j.conbuildmat.2015.12.141

Li L, Wu M (2022) An overview of utilizing CO_2 for accelerated carbonation treatment in the concrete industry. J CO2 Util 60:102000. https://doi.org/10.1016/j.jcou.2022.102000

Liu Z, Meng W (2021) Fundamental understanding of carbonation curing and durability of carbonation-cured cement-based composites: a review. J CO2 Util 44:101428

Marple MAT, Koroglu B, Morrison K et al (2022) Accelerated carbonation and structural transformation of blast furnace slag by mechanochemical alkali-activation. Cem Concr Res 156:106760. https://doi.org/10.1016/j.cemconres.2022.106760

Miraki H, Shariatmadari N, Ghadir P et al (2021) Clayey soil stabilization using alkali-activated volcanic ash and slag. J Rock Mech Geotech Eng 14:576–591. https://doi.org/10.1016/j.jrmge.2021.08.012

Mo L, Zhang F, Deng M (2016) Cement and concrete research mechanical performance and microstructure of the calcium carbonate binders produced by carbonating steel slag paste under CO_2 curing. Cem Concr Res 88:217–226. https://doi.org/10.1016/j.cemconres.2016.05.013

Mortezaei K, Vahedifard F (2015) Numerical simulation of induced seismicity in carbon capture and storage projects. Geotech Geol Eng 33:411–424. https://doi.org/10.1007/s10706-015-9859-7

Naghizadeh A (2019) Mix design and alkali resistance of fly ash geopolymer binders

Norhasyima RS, Mahlia TMI (2018) Advances in CO_2 utilization technology: a patent landscape review. J CO2 Util 26:323–335

Pan SY, Adhikari R, Chen YH et al (2016) Integrated and innovative steel slag utilization for iron reclamation, green material production and CO_2 fixation via accelerated carbonation. J Clean Prod 137:617–631

Park S-S, Le T-T, Nong Z et al (2020) Chemically induced calcium carbonate precipitation for improving strength of sand. J Mater Civ Eng 32:04020238. https://doi.org/10.1061/(asce)mt.1943-5533.0003318

Phoo-Ngernkham T, Maegawa A, Mishima N et al (2015) Effects of sodium hydroxide and sodium silicate solutions on compressive and shear bond strengths of FA-GBFS geopolymer. Constr Build Mater 91:1–8. https://doi.org/10.1016/j.conbuildmat.2015.05.001

Polettini A, Pomi R, Stramazzo A (2016) CO_2 sequestration through aqueous accelerated carbonation of BOF slag: a factorial study of parameters effects. J Environ Manage 167:185–195. https://doi.org/10.1016/j.jenvman.2015.11.042

Praneeth S, Guo R, Wang T et al (2020) Accelerated carbonation of biochar reinforced cement-fly ash composites: Enhancing and sequestering CO_2 in building materials. Constr Build Mater 244:118363. https://doi.org/10.1016/j.conbuildmat.2020.118363

Puertas F, Palacios M (2007) Changes in C–S–H of alkali-activated slag and cement pastes after accelerated carbonation. In: 12th International congress on the chemistry of cement

Razeghi HR, Ghadir P, Javadi AA (2022) Mechanical strength of saline sandy soils stabilized with alkali-activated cements. Sustainability (switzerland). https://doi.org/10.3390/su142013669

Reddy KR, Gopakumar A, Chetri JK (2019) Critical review of applications of iron and steel slags for carbon sequestration and environmental remediation. Rev Environ Sci Biotechnol 18:127–152

Romiani HM, Keykha HA, Talebi M et al (2021) Green soil improvement: using carbon dioxide to enhance the behaviour of clay. Proc Inst Civ Eng: Ground Improv. https://doi.org/10.1680/jgrim.20.00073

Rouaiguia A, El Aal AKA (2020) Enhancement of the geotechnical properties of soils using marble and lime powders, Guelma city, Algeria. Geotech Geol Eng 38:5649–5665. https://doi.org/10.1007/s10706-020-01368-5

Samadi P, Ghodrati A, Ghadir P, Javadi AA (2023) Effect of seawater on the mechanical strength of geopolymer/cement stabilized sandy soils. Proceedings of the TMIC 2022 slope stability conference (TMIC 2022). Atlantis Press International BV, Dordrecht, pp 121–129

Shariatmadari N, Hasanzadehshooiili H, Ghadir P et al (2021) Compressive strength of sandy soils stabilized with alkali-activated volcanic ash and slag. J Mater Civ Eng 33:04021295. https://doi.org/10.1061/(asce)mt.1943-5533.0003845

Silva BA, Ferreira Pinto AP, Gomes A, Candeias A (2021) Effects of natural and accelerated carbonation on the properties of lime-based materials. J CO2 Util 49:101552. https://doi.org/10.1016/j.jcou.2021.101552

Sivapullaiah PV, Jha AK (2014) Gypsum induced strength behaviour of fly ash-lime stabilized expansive soil. Geotech Geol Eng 32:1261–1273. https://doi.org/10.1007/s10706-014-9799-7

Song Q, Guo MZ, Wang L, Ling TC (2021) Use of steel slag as sustainable construction materials: a review of accelerated carbonation treatment. Resour Conserv Recycl 173:105740. https://doi.org/10.1016/j.resconrec.2021.105740

Suescum-Morales D, Bravo M, Silva RV et al (2022) Effect of reactive magnesium oxide in alkali-activated fly ash mortars exposed to accelerated CO_2 curing. Constr Build Mater 342:127999. https://doi.org/10.1016/j.conbuildmat.2022.127999

Syed M, GuhaRay A, Kar A (2020) Stabilization of expansive clayey soil with alkali activated binders. Geotech Geol Eng 38:6657–6677. https://doi.org/10.1007/s10706-020-01461-9

Ukwattage NL, Ranjith PG, Li X (2017) Steel-making slag for mineral sequestration of carbon dioxide by accelerated carbonation. Measurement (lond) 97:15–22. https://doi.org/10.1016/j.measurement.2016.10.057

Vishal V, Singh TN (2015) A laboratory investigation of permeability of coal to supercritical CO_2. Geotech Geol Eng 33:1009–1016. https://doi.org/10.1007/s10706-015-9882-8

Wang D, Zhu J, He F (2019) CO_2 carbonation-induced improvement in strength and microstructure of reactive MgO–CaO-fly ash-solidified soils. Constr Build Mater 229:116914. https://doi.org/10.1016/j.conbuildmat.2019

Wang S, Li X, Ren K, Liu C (2020) Experimental research on steel slag stabilized soil and its application in subgrade engineering. Geotech Geol Eng 38:4603–4615. https://doi.org/10.1007/s10706-020-01313-6

Wang D, Xiao J, Duan Z (2022) Strategies to accelerate CO_2 sequestration of cement-based materials and their application prospects. Constr Build Mater 314:125646. https://doi.org/10.1016/j.conbuildmat.2021.125646

Wong BYF, Wong KS, Phang IRK (2019) A review on geopolymerisation in soil stabilization. In: IOP conference series: materials science and engineering

Yi Z, Wang T, Guo R (2020) Sustainable building material from CO_2 mineralization slag: aggregate for concretes and effect of CO_2 curing. J CO2 Util 40:101196. https://doi.org/10.1016/j.jcou.2020.101196